catalysts

MDPI

Article

Silica Nanoflowers-Stabilized Pickering Emulsion as a Robust Biocatalysis Platform for Enzymatic Production of Biodiesel

Lihui Wang [1,2,†], Xinlong Liu [2,†], Yanjun Jiang [1], Peng Liu [2], Liya Zhou [1], Li Ma [1], Ying He [1], Heyu Li [3] and Jing Gao [1,*]

[1] School of Chemical Engineering, Hebei University of Technology, No. 8 Guangrong Road, Hongqiao District, Tianjin 300130, China; wanglihui81@yeah.net (L.W.); yanjunjiang@hebut.edu.cn (Y.J.); liyazhou@hebut.edu.cn (L.Z.); malihgd@yeah.net (L.M.); heying1980@hebut.edu.cn (Y.H.)

[2] Department of Biochemical Engineering, Tianjin Modern Vocational Technology College, No. 3 Yaguan Road, Jinnan District, Tianjin 300350, China; wanglihui81@yeah.net (L.W.); liuxl88@yeah.net (X.L.); xdliupeng@yeah.net (P.L.)

[3] Tianjin Ubasio Biotechnology Group Co., Ltd., Tianjin 300457, China; liheyu19@yeah.net

* Correspondence: jgao@hebut.edu.cn; Tel.: +86-226-020-4293

† These authors contributed equally to this work.

Received: 15 October 2019; Accepted: 30 November 2019; Published: 4 December 2019

Abstract: Enzymatic production of biodiesel had attracted much attention due to its high efficiency, mild conditions and environmental protection. However, the high cost of enzyme, poor solubility of methanol in oil and adsorption of glycerol onto the enzyme limited the popularization of the process. To address these problems, we developed a silica nanoflowers-stabilized Pickering emulsion as a biocatalysis platform with *Candida antarctica* lipase B (CALB) as model lipase for biodiesel production. Silica nanoflowers (SNFs) were synthesized in microemulsion and served as a carrier for CALB immobilization and then used as an emulsifier for constructing Pickering emulsion. The structure of SNFs and the biocatalytic Pickering emulsion (CALB@SNFs-PE) were characterized in detail. Experimental data about the methanolysis of waste oil to biodiesel was evaluated by response surface methodology. The highest experimental yield of 98.5 ± 0.5% was obtained under the optimized conditions: methanol/oil ratio of 2.63:1, a temperature of 45.97 °C, CALB@SNFs dosage of 33.24 mg and time of 8.11 h, which was closed to the predicted value (100.00%). Reusability test showed that CALB@SNFs-PE could retain 76.68% of its initial biodiesel yield after 15 cycles, which was better than that of free CALB and N435.

Keywords: pickering emulsion; silica nanoflowers; biodiesel; response surface methodology

1. Introduction

Over the last decades, alternative fuels for internal combustion engines have attracted considerable attention. Biodiesel, which refers to short-chain esters of fatty acid, is an attractive energy thanks to its renewable, safe, biodegradable and eco-friendly properties [1]. Moreover, the much similar properties of cetane number, energy content, viscosity and phase changes with fossil fuels, biodiesel can be directly used by the existing fuel engines, vehicles, and infrastructure without any pretreatment [2,3].

Generally, biodiesel can be synthesized by esterification or transesterification of short-chain alcohols with various oils (jatropha oil, rapeseed oil, waste oil, etc.) in the presence of a catalyst. Conventional catalysts were various chemicals (acid and base). However, the chemical-catalyzed

process suffered from several drawbacks such as high energy requirements, chemicals, corrosion damage to equipment, and complex product purification process [3,4]. Subsequently, the enzyme was triggered as biocatalysts in the production of biodiesel. Enzymatic synthesis of biodiesel, especially using immobilized enzyme as a catalyst, has greater advantages including high efficiency, low energy consumption, simple process and fewer by-products [5,6]. However, the reaction efficiency of biocatalytic processes is usually hampered by the facts: the oils are only soluble in organic phase while enzymes are usually more active in the aqueous environment and the presence of water, in turn, inhibited the synthesis of biodiesel [7–9], limited reaction interfacial area and high mass transport resistance [10,11]. In addition, The enzymes were often damaged caused mainly by the use of methanol as substrate [12,13] and partly by the glycerol generated [14,15]. Pickering emulsion, stabilized by solid particles, provides a simple and feasible solution to solve these obstacles. In this system, substrates and enzymes can be in their own comfortable microenvironment without any interference, but they can work together to promote biodiesel production. Pickering emulsion systems owned a large interface area and short molecule diffusion distance [16], which enable biphasic reactions to proceed efficiently and simplify catalyst recovery operations [11,17–20]. Now, Pickering emulsion stabilized by hybrid nanoparticles, periodic mesoporous silica encapsulated with lipase [21] or carbon nanotubes crosslinked with lipase [22], have been constructed and used in enzymatic reactions [23,24]. All the reported systems showed enhanced catalytic activity, stability, and reusability compared to the native enzymes.

Silica nanoflowers (SNFs), a kind of porous silica material with center-radial pore structure, have garnered a great deal of attention in the last years. The variety and ease of control structures (sizes, connective and external morphology) attributed to the use of the substructures of microemulsions as templates further expanded its application range of SNFs [25,26]. Especially in the field of enzyme catalysis, the high accessibility to guests and large surface area of SNFs due to its unique open-pore superstructures can facilitate the enzyme molecules loading in them and the mass transfer of substrates, which is beneficial for the improvement of catalytic activity and products yield [27,28]. Until now, many researchers had used SNFs as a carrier for enzyme immobilized and utilized in hydrogenolysis [29], dehydration [30], reduction [31], and transesterification [32]. Yan's group [33] constructed a kind of carbon nanotube-lipase hybrid nanoflowers and the new immobilized lipase exhibited 68-fold higher activity relative to free lipase in the esterification of lauric acid and 1-dodecanol. Zhao et al. [34]reported an application of a dual-enzyme nanoflower that exhibiting a much higher catalytic performance than the free enzymes in cascade epoxidation. After the catalyst was reused for 10 times, the yield of epoxidation was still 82%, which indicated its good reusability. The same conclusion could be reached in many other pieces of literature that SNFs can be more efficient to improve the enzyme activity and stability [27]. However, to the best of our knowledge, the catalytic system that combines the advantage of silica nanoflowers and Pickering emulsion has not been reported.

Waste oils, the inferior oil such as recycled cooking oil and repeatedly used frying oil existing in life, have no direct utility value and are extremely harmful to human health. In order to make rational use of waster oil, many researchers have converted them into biodiesel by using acid catalyst [35], lipase [4,36], or other catalysts [37,38]. As far as we know, there have been rare reports on the catalytic synthesis of biodiesel from waste oil by using silica nanoflowers-stabilized Pickering emulsion as a biocatalysis platform.

Thus, herein, a silica nanoflowers-stabilized Pickering emulsion was constructed as a robust interfacial biocatalytic platform for biodiesel production from waste oil. The silica nanoflowers were prepared in the bicontinuous microemulsion phase of the Winsor III system according to our previous report, and then the obtained silica nanoflowers were modified by dichlorodimethylsilane for the adsorption of *Candida antarctica* lipase B (CALB). The obtained immobilized CALB particles (silica nanoflowers) were used to construct biocatalytic Pickering emulsion and then used in the production of biodiesel. Method of response surface methodology (RSM) was employed to optimize the biodiesel production process and the influence of four variables (molar ratio of methanol to oil, temperature, enzymatic dosage, and reaction time) were examined. The optimum conditions for

obtaining the highest biodiesel yield were studied and predicted through a quadratic polynomial equation [39]. Finally, the stability of the biocatalytic Pickering emulsion was investigated.

2. Results and Discussion

2.1. Characterization

The morphologies of the SNFs are shown in Figure 1a,b. The scanning electron microscopy (SEM) image revealed that SNFs were spherical particles with a uniform diameter of 0.5 μm and porous surface structures. From the transmission electron microscopy (TEM) image, a 3D center-radial open structure of SNFs was clearly described. The open dendritic superstructures could provide a huge accessible internal surface area, which was beneficial for the transfer of lipase molecules and substrates [27]. Figure 2a showed the N_2 adsorption-desorption isotherms of SNFs and CALB@SNFs. Both the adsorption isotherms exhibited a sharp increase of P/P_0 from 0.8 to 1.0 with a hysteresis loop at $0.4 < P/P_0 < 1.0$ (type H_1), indicating the center-radial channels were mesoporous. The corresponding pore size distribution was calculated by the Barrett-Joyner-Halenda theory (Figure 2b). A unimodal pore width distribution centered on 3.1 nm was obtained, which was consistent with the above conclusion of mesoporous structure. The specific surface area change of SNFs before and after lipase immobilization was determined by Brunauer-Emmett-Teller derived from the isotherms. The pore volume of SNFs (0.9317 cm^3/g) decreased to 0.6764 cm^3/g, and the specific surface area decreased from 624.9 m^3/g to 410.9 m^3/g, illustrating that lipase was loaded on the SNFs. In order to further identify whether the lipase was immobilized on SNFs or not, infrared spectra of SNFs and CALB@SNFs were obtained. Peaks at 966, 879, 1554 cm^{-1} aroused from amido bonds stretching vibration were the characteristic peaks of lipase [40]. As shown in Figure 3, the characteristic peaks only appeared in the spectra of CALB@ SNFs, but not in the SNFs spectrum, which confirmed that lipase was successfully immobilized onto the SNFs [41].

Figure 4a revealed that CALB@SNFs-PE consisted of a number of small spheres with good dispersion and stable state. The droplet size was in the range of 30–40 μm. FITC-DEX was a fluorescent that dissolves only in the aqueous phase and its distribution in CALB@SNFs-PE was recorded in Figure 4b. The appearance of green fluorescence inside each sphere indicated that CALB@SNFs-PE owned water-in-oil structure, which was conducive to the separation of products in the process of biodiesel production.

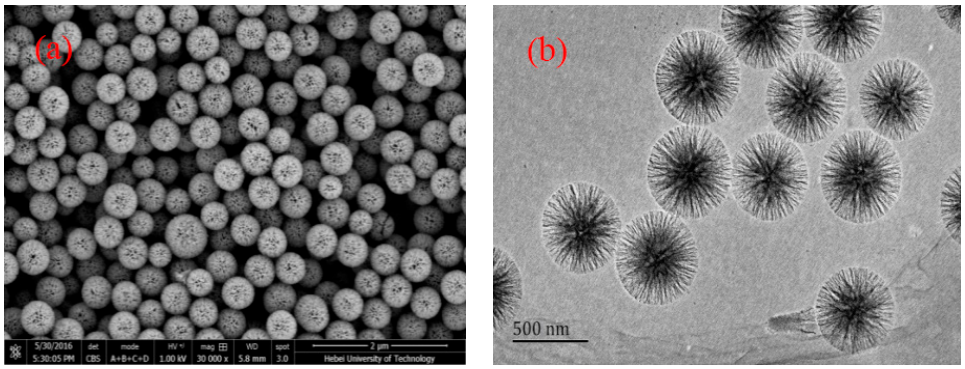

Figure 1. (**a**) SEM and (**b**) TEM image of SNFs.

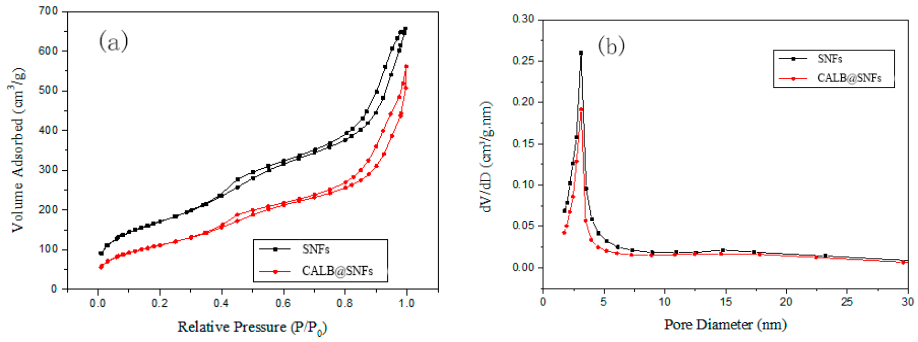

Figure 2. (**a**) Nitrogen adsorption-desorption isotherms of SNFs and CALB@SNFs; (**b**) Pore size distribution profile of SNFs.

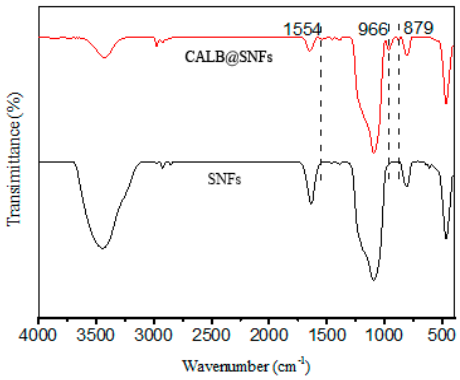

Figure 3. Infrared spectra analysis of SNFs and CALB@SNFs.

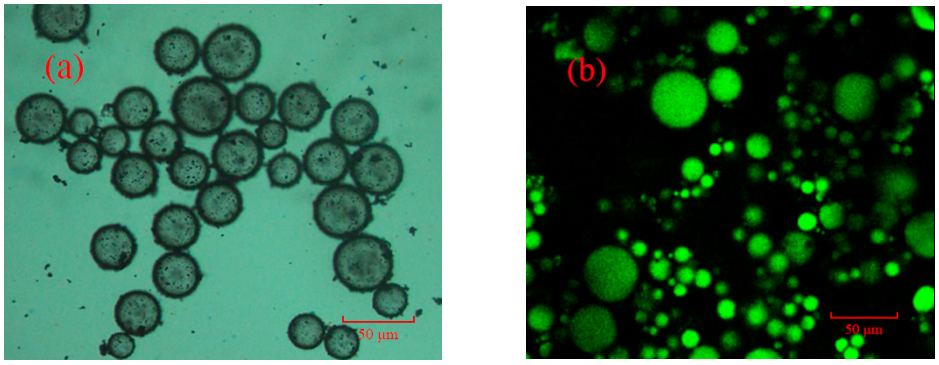

Figure 4. (**a**) Optical microscope image of CALB@SNFs-PE droplets; (**b**) CLSM image of CALB@SNFs-PE with FITC-Dex in water (495–545 nm).

2.2. Optimization of Biodiesel Production through CCD

Four biodiesel production process parameters, i.e., the molar ratio of methanol to oil, CALB@SNFs dosage, temperature and time were optimized using central composite design. Tables 1 and 2 represented the range of components and each experimental design for central composite design (CCD) in detail. As can be seen, the biodiesel yield varied from 41.70% to 99.00% and was affected by the variation of the four conditions. These interactions were analyzed and calculated through Analysis of Variance (ANOVA) using Design Expert 8.0.6. According to the statistical analysis results, a polynomial quadratic equation was established by the RSM software (Table 3). The model Equation (1) described the biodiesel yield (Y) as a function of the molar ratio of methanol to oil (A), temperature (B), CALB@SNFs dosage (C) and time (D). The positive coefficient of the item had a positive effect on yield increasing, while negative sign accounted for antagonistic effect [42].

Table 4 indicated the analysis results of ANOVA that could be employed to evaluate the significance of the model and each item as well as their interaction on biodiesel yield. In this case, the

model F value for biodiesel yield was 729.79 with p-value < 0.0001 suggested the model was extremely significant for the biodiesel production. The probability that a "Model F-Value" was not significant due to noise disturbance is only 0.01%. In addition, the main model items with significant influence on biodiesel yield were the molar ratio of methanol to oil (A), temperature (B), CALB@SNFs dosage (C), time (D) and their quadratic terms, while the interaction terms existed in AD, AC, BD, and CD. To be clear, factors A and D were significant and the interaction was not significant. This phenomenon may be caused by an indirect correlation between them caused by unknown factors.

$$\text{Yield}(\%) = 97.13 - 8.27A - 4.26\,B + 6.62\,C + 3.99\,D - 5.06\,AB + 3.01\,AC - 0.66\,BC - 3.38\,BD - 1.53\,CD - 9.65A^2 - 6.24\text{B}^2 - 3.59\,C^2 - 1.15\,D^2 \quad (1)$$

The goodness of fit of the model equation should be evaluated before it was used to predict the actual biodiesel yield. The determination coefficient (R^2) of 0.9985 and adjusted determination coefficient (Adj-R^2) of 0.9972 both showed the better aptness of the model. Meanwhile, the "Pred-R^2" of 0.9929 was in reasonable agreement with the "Adj-R^2" further suggested that the equation had better regression and fitting degree. Non-significant "lack of fit" (p = 0.2704) further indicated that the fitting between model and experimental data was satisfactory (Figure 5a). The applicability of the equation could also be analyzed using the plot of residuals versus predicted response (Figure 5b). Irregular distribution of data suggested the model was adequate and no violation of independence or constant variance assumption existed in the model [42]. Figure 5c showed the normal probability plot of the residuals. The data distributed normally in straight approximate lines indicated that the errors were insignificant. The simultaneous effect of all the factors on the yield was shown in Figure 5d. The perturbation graph revealed that the production process was most sensitive to CALB@SNFs dosage and least affected by the molar ratio of methanol to oil.

Table 1. Central composite design (CCD) of independent variables and levels.

Systems	Independent Variables	Unit	Low Level (–)	High Level (+)	–Alpha	+Alpha
A	Molar ratio of methanol to oil		2	4	1	5
B	Temperature	℃	37.5	52.5	30	60
C	CALB@SNFs dosage	mg	20	40	10	50
D	Time	h	6	10	4	12

Table 2. Experimental design and yield of biodiesel production using CCD-RSM.

NO.	Type	A (Molar Ratio of Methanol to Oil)	B (Temperature, °C)	C (CALB@SNFs Dosage, mg)	D (Time, h)	Yield %
1	Factorial	2.00	37.50	20.00	6.00	70.55
2	Factorial	4.00	37.50	20.00	6.00	58.62
3	Factorial	2.00	52.50	20.00	6.00	80.20
4	Factorial	4.00	52.50	20.00	6.00	48.59
5	Factorial	2.00	37.50	40.00	6.00	82.31
6	Factorial	4.00	37.50	40.00	6.00	81.66
7	Factorial	2.00	52.50	40.00	6.00	89.38
8	Factorial	4.00	52.50	40.00	6.00	68.93
9	Factorial	2.00	37.50	20.00	10.00	89.63
10	Factorial	4.00	37.50	20.00	10.00	76.10
11	Factorial	2.00	52.50	20.00	10.00	86.00
12	Factorial	4.00	52.50	20.00	10.00	52.30
13	Factorial	2.00	37.50	40.00	10.00	94.25
14	Factorial	4.00	37.50	40.00	10.00	94.09
15	Factorial	2.00	52.50	40.00	10.00	88.50
16	Factorial	4.00	52.50	40.00	10.00	67.09
17	Axial	1.00	45.00	30.00	8.00	74.26
18	Axial	5.00	45.00	30.00	8.00	41.70
19	Axial	3.00	30.00	30.00	8.00	80.66
20	Axial	3.00	60.00	30.00	8.00	62.60
21	Axial	3.00	45.00	10.00	8.00	68.59

22	Axial	3.00	45.00	50.00	8.00	95.90
23	Axial	3.00	45.00	30.00	4.00	84.95
24	Axial	3.00	45.00	30.00	12.00	99.00
25	Center	3.00	45.00	30.00	8.00	97.70
26	Center	3.00	45.00	30.00	8.00	96.70
27	Center	3.00	45.00	30.00	8.00	97.10
28	Center	3.00	45.00	30.00	8.00	97.80
29	Center	3.00	45.00	30.00	8.00	95.97
30	Center	3.00	45.00	30.00	8.00	97.50

Table 3. Sequential Model Sum of Squares (Type I).

Source	Sum of Squares	Mean Square	F Value	Prob>F	
Mean	195000	1950			
Liner	3512.87	878.22	5.34	0.0030	
2FI	782.17	130.36	0.74	0.6216	
Quadratic	3319.69	829.92	1113.56	<0.0001	Suggested
Cubic	5.23	0.65	0.77	0.6427	Aleased
Residual	5.95	0.85			
Total	202600	6753.95			

Table 4. Analysis of variance for the yield of biodiesel.

Terms	Sum of Squares	F-Value	*p*-Value (Prob>F)	Analysis
Model	7614.72	729.79	<0.0001	significant
A: Molar ratio of methanol to oil	1642.88	2204.35	<0.0001	
B: Temperature	436.35	585.48	<0.0001	
C: CALB@SNFs dosage	1051.11	1410.33	<0.0001	
D: Time	382.53	513.26	<0.0001	
AB	409.04	548.83	<0.0001	
AC	144.52	193.91	<0.0001	
AD	1.08	1.45	0.2470	
BC	7.04	9.44	0.0077	
BD	183.23	245.85	<0.0001	
CD	37.26	49.99	<0.0001	
A^2	2555.77	3429.23	<0.0001	
B^2	1.68.11	1433.14	<0.0001	
C^2	352.85	473.44	<0.0001	
D^2	36.54	49.33	<0.0001	
Residual	11.18	0.75		
Lack of Fit	8.74	1.79	0.2704	not significant
Pure Error	2.44	0.49		
Standard of deviation	0.86		R^2	0.9985
Mean	80.62		Adjusted R^2	0.9972
Coefficient of variation %	1.07		Predicted R^2	0.9929
PRESS	53.84		Adequate Precision	95.876

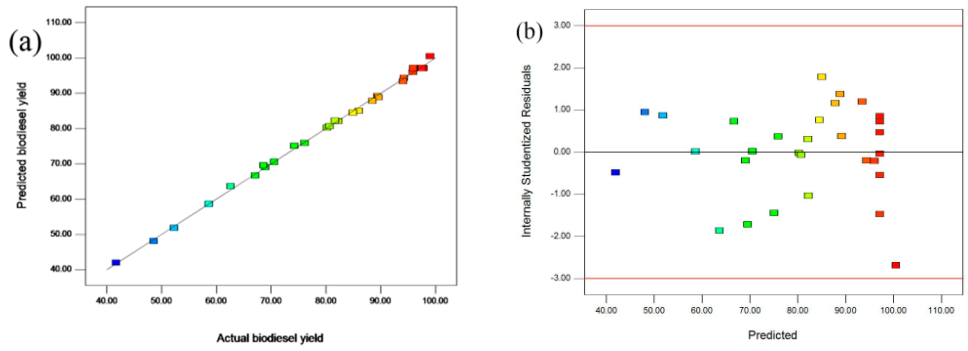

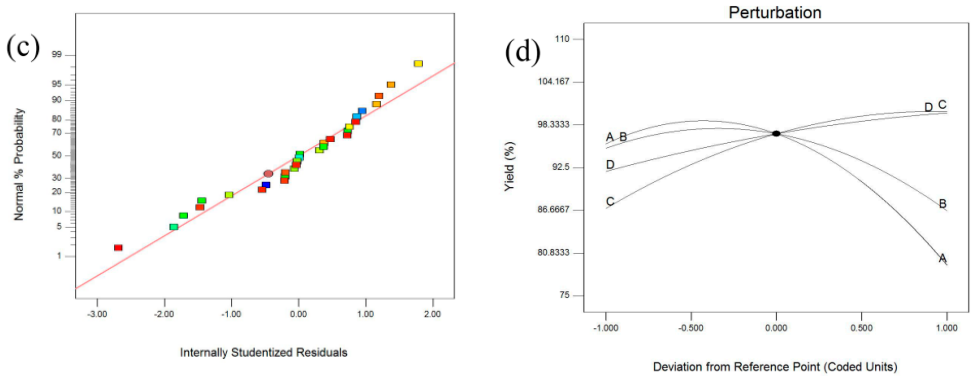

Figure 5. (**a**) predicted versus experimental biodiesel yield; (**b**) plot of the residuals versus the predicted response; (**c**) normal probability plots of residuals; (**d**) perturbation plot showing the influence of variables on biodiesel yield.

2.3. Parameters Study and Interaction Between Independent Variable

The 3D surfaces and contour curves of biodiesel yield from methanolysis of waste oil were analyzed to measure the interaction between two variables and determine the optimum conditions for maximum yield. Figure 6a illustrated the cumulative effect of the molar ratio of methanol to oil and CALB@SNFs dosage meanwhile keeping other factors at the "0" level. It showed that increment of methanol to oil molar ratio initially led to a slight increase of biodiesel yield and then rapidly decline at the higher level of CALB@SNFs dosage. Biodiesel yield increased proportionately when CALB@SNFs dosage was increased. As we all know, the more catalyst, the faster the reaction. And the presence of a large number of particles was conducive to increase the specific surface area of emulsion droplets, which could enhance the catalytic activity of CALB [21]. Figure 6b revealed that the increment of molar ratio of methanol to oil from the central level to a higher level caused a decrease in biodiesel yield. Excessive methanol would break the molecular structure of the enzyme, resulting in its loss of catalytic capacity. On the contrary, the yield was slightly influenced by the raise of time. This might be caused by exhausted substrates. Figure 6c reveals the variation of yield with temperature and time. It clearly showed that the biodiesel yield reduced when the temperature was increased or decreased beyond the central level. However, increasing the reaction time affected the yield a little. Therefore, maximum response value was obtained close to + 1 level of time at 0 level of temperature. The influence of CALB@SNFs dosage and time on biodiesel yield was shown in Figure 6d. Either CALB@SNFs dosage or time exhibited the same trends with the yield, showing a strong interaction effect as indicated by the elliptical contour plot [43].

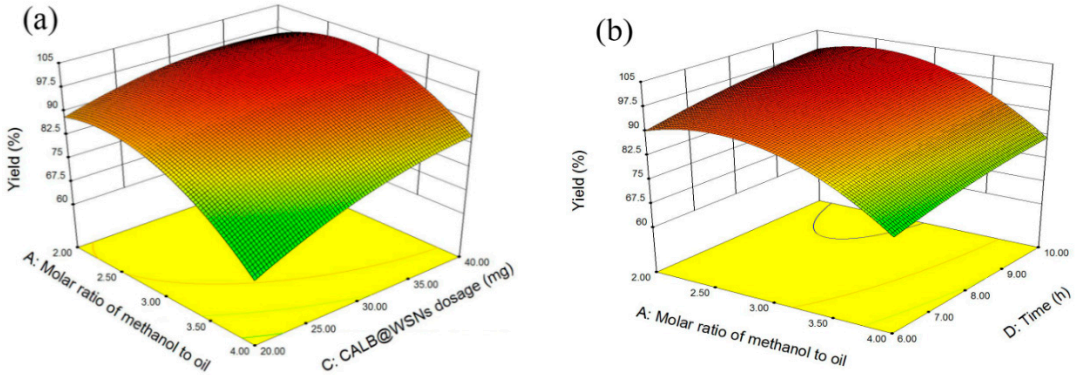

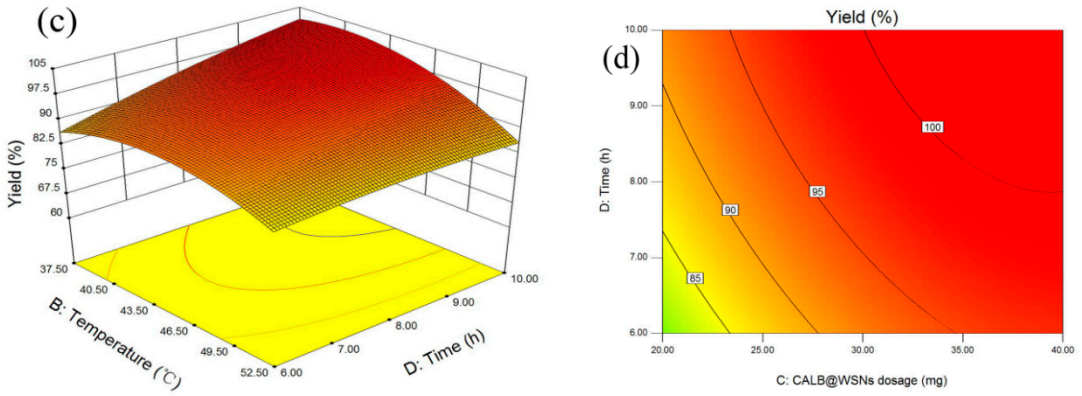

Figure 6. 3D surfaces and contour curve showing cumulative effect of two variables on the yield of biodiesel (**a**) interaction between molar ratio of methanol to oil and CALB@SNFs dosage; (**b**) interaction between molar ratio of methanol to oil and Time; (**c**) interaction between Temperature and Time; (**d**) interaction between CALB@SNFs dosage and Time.

2.4. Validation of the Model

Based on the CCD and ANOVE results, a model (Equation (1)) was employed to determine the optimum conditions composition of biodiesel yield. To validate the proposed model, several experiments, whose conditions belonged to the range of variables, were performed and each experiment was repeated three times. The reaction conditions and biodiesel yields for each reaction were listed in Table 5. From the table, the corresponding yield obtained was much closer to the predicted value by model. For biodiesel production enterprises, obtaining the maximum yield was one of the most important goals, which was chosen as the criterion for determining the best process conditions combination in this section. Based on this constraint, the optimized conditions for maximum biodiesel yield were shown as follows: molar ratio of methanol to oil 2.63: 1, temperature 45.97 °C, CALB@SNFs dosage 33.24 mg, time 8.11 h. The experimental yield was 98.5 ± 0.5% and the theoretical value was 100.00% calculated by the proposed model. Thus, the almost identical results could confirm that the CCD model was accurate and reliable for predicting the biodiesel yield within the range of parameters selected by the experimental design.

Table 5. The validated experimental results of model at the optimum conditions.

Solution	Molar Ratio of Methanol to Oil	Temperature, °C	CALB@SNFs Dosage, mg	Time, h	Theoretical Yield %	Experimental Yield %
1	2.63	45.97	33.24	8.11	100.00	98.5 ± 0.6
2	2.97	44.15	30.24	9.15	99.99	98.3 ± 0.4
3	2.34	38.02	39.23	9.89	99.99	98.2 ± 0.7

2.5. Performance Comparison of Free CALB, N435 and CALB@SNFs-PE

N435 was a widely applied commercial lipase and commonly used to evaluate the practicality of catalyst. In this case, the catalytic performance and reusability of free CALB, N435 and CALB@SNFs-PE with equal protein was determined under the above optimum conditions. As can be seen in Figure 7a, the maximum biodiesel yield was 98.8% catalyzed by CALB@SNFs-PE, which was twice over that of N435 (47.78%) and nearly four times than that of free CALB (24.09%). This result indicated that the Pickering emulsion system was more favorable for esterification and transesterification for biodiesel production. The significant advantage might be attributed to the following points: (1) the microenvironment at the phase interface was more conducive to the formation or exposure of lipase activity sites; (2) the unique structure of SNFs was beneficial to the diffusion of substrate molecules and contact with CALB molecules.

The reusability of CALB@SNFs-PE was a key parameter that affects the industry application. Figure 7b showed the relative yields of biodiesel with free CALB, N435 or CALB@SNFs-PE as the catalyst. The biodiesel yield of the first cycle was defined as 100%. After repeated use for 15 times, the yields of biodiesel catalyzed by N435 and CALB@SNFs-PE were 24.34% and 76.68%, respectively. While the yield catalyzed by free CALB was almost zero. This result revealed that immobilization could effectively improve the stability of lipase molecules. The CALB@SNFs-PE was more stable than N435 might because of the better stability of SNFs than that of the resin used in Novozym 435. Beyond that, lipase preferred to rest at the phase interface, which made it harder to detour from particles at the interface. However, N435 gradually broke up with the used number increase, and the contained enzyme molecules were lost to the solvent, which might be the cause of the poor reusability of N435. The changes in particle morphology of N435 were visible and the desorption of the lipase could be confirmed by measuring the change of protein content in the solution.

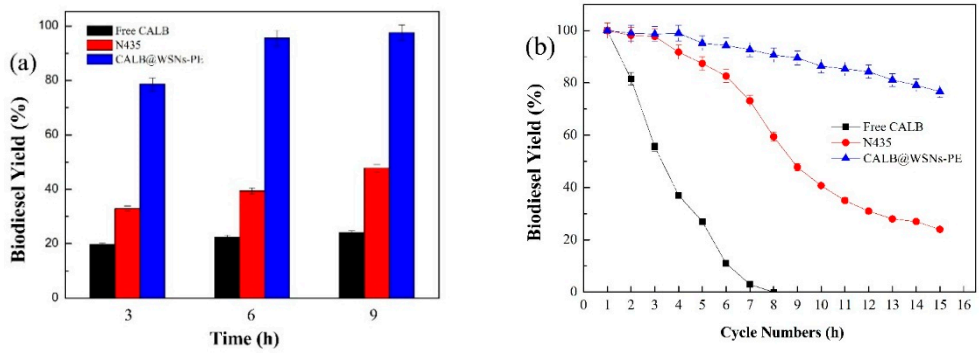

Figure 7. The catalytic performance (**a**) and reusability (**b**) of free CALB, N435 and CALB@SNFs-PE with equal protein in biodiesel production (molar ratio of methanol to oil 2.72:1, Temperature 43.89 °C, CALB@SNFs dosage 32.40 mg, Time 7.92 h).

3. Materials and Methods

3.1. Material

The *Candida antarctica* lipase B (16.7 mg protein/mL) and Novozym 435 were purchased from Beijing Cliscent Technology Co., Ltd. (Beijing, China). Cetyltrimethylammonium bromide (CTAB) and tetraethylorhtosilicate (TEOS) were purchased from Shanghai Aladdin Bio-Chem Technology Co., LTD (Shanghai, China). Dichlorodimethylsilane and fluorescein isothiocyanate (FITC) was purchased from Tokyo Chemical Industry Co., Ltd. (Tokyo, Japan). N-Butanol, cyclohexane, toluene, ethanol, urea, oleic acid and methanol were purchased from Damao Chemical Reagent Factory (Tianjin, China). Other chemicals were all purchased from Sigma-Aldrich (Shanghai, China).

3.2. Synthesis of the Silica Nanoflowers

For the synthesis of SNFs, CTAB (1.0 g) was mixed with n-butanol (1.0 g), urea aqueous solution (0.4 mol/L, 30 g), cyclohexane (12 g) in the 100 mL round flask and oscillated for 30 min. Then, TEOS (2 g) was dropwise added into the mixture under stirring at 25 °C. After 30 min, the system temperature was raised to 70 °C and kept for 20 h. After that, the precipitate was collected by centrifugation and washed with ethanol for three times. Finally, the SNFs were obtained by calcining at 550 °C in a resistance furnace for 5 h [25,44,45].

The silica nanoflowers were modified by dichlorodimethylsilane. Briefly, the silica nanoflowers (1 g) were mixed with dichlorodimethylsilane (0.5 mL) in toluene (100 mL) and reacted for 20 h at room temperature under stirring condition. Then the modified silica nanoflowers were obtained through centrifugation and washing by toluene and ethanol in turn.

3.3. Construction of the Biocatalytic Pickering Emulsion

Firstly, the modified silica nanoflowers were used as a carrier to immobilize CALB by adsorption method. An amount of 15 mg modified silica nanoflowers were dispersed into 1.75 mL CALB solution and then mixed with 3.25 mL PBS (Phosphate Buffer solution, 10 mM, pH 7.0). After 2 h of adsorption, the product was centrifuged and washed with PBS for three times. The obtained immobilized CALB (named as CALB@SNFs) was freeze-dried and employed as the stabilizer for constructing biocatalytic Pickering emulsion. Under this condition, the immobilization capacity of SNFs was 81 mg protein/g SNFs and the activity recovery was 14.8% [46].

Secondly, 20 mg CALB@SNFs was injected into a pressure bottle containing cyclohexane (5 mL) and ultrasonic oscillated for 5 min using BILON-250Y (12 W, 1 s/3 s intervals). Then, 1.5 mL PBS was added into the mixture followed by another 10 min ultrasonic emulsification. After the operation, the biocatalytic Pickering emulsion was prepared and named CALB@SNFs-PE. All the experiment parameters, such as CALB@SNFs dosage, PBS volume and ultrasonic time, were the optimal values after experimental optimization, which would be reported in our follow-up paper.

3.4. Characterization

Morphology of SNFs was observed by scanning electron microscopy (SEM) and transmission electron microscopy (TEM) using Hitachi S4800 and H-7600 instruments (Tokyo, Japan), respectively. The N_2 adsorption-desorption isotherms and the pore-size distributions of SNFs and CALB@SNFs were all measured at 77 K with a Micromeritics ASAP 2020M (Norcross, GA, USA). Infrared spectra were measured using a Brukervector/22 FTIR spectrometer to determine whether lipase was immobilized onto SNFs.

An optical microscope was utilized to observe the Morphology of CALB@SNFs-PE. In order to determine the type of Pickering emulsion, PBS was mixed with FITC-Dex and then used as the aqueous phase for emulsion preparation. The labelled CALB@SNFs-PE was observed by confocal laser scanning microscopy (CLSM, Leica TCS SP5 optical microscope) with the emission of 495–545 nm [9,47,48].

3.5. Production of Biodiesel

The reaction of biodiesel production was performed in a 15 mL screw-capped vessel containing waste oil (1.5 g), methanol (molar ratio of methanol to oil of 1:1 to 5:1) and CALB@SNFs-PE (CALB@SNFs dosage was 10 mg–50 mg). The mixtures were incubated in an electro-thermostatic water bath (90 r/min) at certain temperatures (ranging from 30 °C to 60 °C) for a certain time. The yield of biodiesel was monitored by gas chromatography (GC) using FID as a detector. DB-5 capillary column (15 m × 0.320 mm) was served as stationary phases and nitrogen (20 mL/min) was used as a mobile phase. The gasify room and the detector temperature were set as 230 °C and 260 °C, respectively. The temperature program of GC column could be divided into four stages: initial temperature of 160 °C for 2 min; rose to 220 °C within 4 min; heated up to 260 °C at 8 °C min^{-1}; keeping temperature until the end. The biodiesel yield of each sample taken at a different time was determined through an internal standard method [49].

The biodiesel production process was analyzed using CCD-RSM providing by Design Expert 8.0.6. A four-factor-five-level with 30 experiments containing 6 same center points, 8 axial points, and 16 factorial points were designed in this study. The center points repeating 6 times were to measure the experimental pure error and enhance the accuracy of data. The four factors their level values based on our previous research were A: molar ratio of methanol to oil (1:1, 2:1, 3:1, 4:1, 5:1), B: temperature (30 °C, 37.5 °C, 45 °C, 52.5 °C, 60 °C), C: CALB@WSN dosage (10 mg, 20 mg, 30 mg, 40 mg, 50 mg) and D: time (4 h, 6 h, 8 h, 10 h, 12 h) (Table 1). The 30 experiments were randomly conducted with the intention to minimize errors from the systematic trends [4].

The reusability of CALB@SNFs-PE was evaluated by examining the biodiesel yield in each cycle of the reaction. After each reaction cycle, most cyclohexane (95%) was removed after static stratification and the rest of the system was rinsed several times with equal volume fresh solvents.

New substrates of the equal amount consumed in the previous round were introduced into the system again for the next reaction [9]. During this process, there was no deactivation of CALB@SNFs that occurred by experimental determination.

4. Conclusions

In the current research, a robust biocatalytic Pickering emulsion was successfully constructed using silica nanoflowers containing CALB as an emulsifier and then applied to catalyze biodiesel production from waste oil and methanol. CCD and RSM were used to study the effects of four factors, methanol/oil ratio, temperature, CALB@SNFs dosage and time on the biodiesel yield. A statistical mode obtained by multiple regression analysis predicted that the highest biodiesel yield would be 100.07% at the following optimized combinations: methanol/oil of 2.63:1, the temperature of 45.97 °C, CALB@SNFs dosage of 33.24 mg and time of 8.11 h. The actual experimental yield at the same conditions was 98.5 ± 0.5%, which was in agreement with the predicted value. Reusability test showed that CALB@SNFs-PE could remain a stable function and structure even after 15 cycles, which provided a robust platform for biodiesel production.

Author Contributions: Conceptualization, Y.J. and J.G.; Data curation, X.L. and Y.J.; Funding acquisition, L.W. and J.G.; Investigation, L.W. and P.L.; Project administration, L.W. and Y.J.; Resources, L.W.; Software, X.L.; Writing—original draft, X.L. and L.Z.; Writing—review & editing, L.M. Y.H. and H.L.

Funding: This research and the APC were both funded by the Tianjin Jinnan District Science and Technology Project (grant number: 20161515).

Conflicts of Interest: The authors declare no conflict of interest.

References

1. Karmakar, B.; Halder, G. Progress and future of biodiesel synthesis: Advancements in oil extraction and conversion technologies. *Energy Convers. Manag.* **2019**, *182*, 307–339.
2. Abed, K.A.; Gad, M.S.; El Morsi, A.K.; Sayed, M.M.; Elyazeed, S.A. Effect of biodiesel fuels on diesel engine emissions. *Egypt. J. Pet.* **2019**, *28*, 183–188.
3. Christopher, L.P.; Hemanathan, K.; Zambare, V.P. Enzymatic biodiesel: Challenges and opportunities. *Appl. Energy* **2014**, *119*, 497–520.
4. Babaki, M.; Yousefi, M.; Habibi, Z.; Mohammadi, M. Process optimization for biodiesel production from waste cooking oil using multi-enzyme systems through response surface methodology. *Renew. Energy* **2017**, *105*, 465–472.
5. Nielsen, P.; Brask, J.; Fjerbaek Søtof, L. Enzymatic biodiesel production: Technical and economical considerations. *Eur. J. Lipid Sci. Technol.* **2008**, *110*, 692–700.
6. You, Q.; Yin, X.; Zhao, Y.; Zhang, Y. Biodiesel production from jatropha oil catalyzed by immobilized Burkholderia cepacia lipase on modified attapulgite. *Bioresour. Technol.* **2013**, *148*, 202–207.
7. Tsai, S.; Chang, C. Kinetics of lipase-catalyzed hydrolysis of lipids in biphasic organic—Aqueous systems. *J. Appl. Chem. Biotechnol.* **1993**, *57*, 147–154.
8. Zaks, A.; Klibanov, A.M. Enzymatic catalysis in nonaqueous solvents. *J. Biol. Chem.* **1988**, *263*, 3194–3201.
9. Wang, Z.; Oers, M.C.M.; Floris, R.P.J.T.; Hest, V.J.C.M. Polymersome Colloidosomes for Enzyme Catalysis in a Biphasic System. *Angew. Chem. Int. Ed.* **2012**, *51*, 10746–10750.
10. Stepankova, V.; Bidmanova, S.; Koudelakova, T.; Prokop, Z.; Chaloupkova, R.; Damborsky, J. Strategies for Stabilization of Enzymes in Organic Solvents. *ACS Catal.* **2013**, *3*, 2823–2836.
11. Wei, L.; Zhang, M.; Zhang, X.; Xin, H.; Yang, H. Pickering Emulsion as an Efficient Platform for Enzymatic Reactions without Stirring. *ACS Sustain. Chem. Eng.* **2016**, *4*, 6838–6843.
12. Nguyen, H.C.; Liang, S.H.; Doan, T.T.; Su, C.H.; Yang, P.C. Lipase-catalyzed synthesis of biodiesel from black soldier fly (Hermetica illucens): Optimization by using response surface methodology. *Energy Convers. Manag.* **2017**, *145*, 335–342.
13. Bandikari, R.; Qian, J.; Baskaran, R.; Liu, Z.; Wu, G. Bio-affinity mediated immobilization of lipase onto magnetic cellulose nanospheres for high yield biodiesel in one time addition of methanol. *Bioresour. Technol.* **2018**, *249*, 354–360.

14. Shahedi, M.; Yousefi, M.; Habibi, Z.; Mohammadi, M.; As'habi, M.A. Co-immobilization of Rhizomucor miehei lipase and Candida antarctica lipase B and optimization of biocatalytic biodiesel production from palm oil using response surface methodology. *Renew. Energy* **2019**, *141*, 847–857.
15. Mohammadi, M.; Ashjari, M.; Dezvarei, S.; Yousefi, M.; Babaki, M.; Mohammadi, J. Rapid and high-density covalent immobilization of Rhizomucor miehei lipase using a multi component reaction: Application in biodiesel production. *RSC Adv.* **2015**, *5*, 32698–32705.
16. Zhang, W.; Fu, L.; Yang, H. Micrometer-Scale Mixing with Pickering Emulsions: Biphasic Reactions without Stirring. *ChemSusChem* **2014**, *7*, 391–396.
17. Yang, B.; Leclercq, L.; Clacensb, J.M.; Rataj, V.N. Acidic/amphiphilic silica nanoparticles: New eco-friendly Pickering interfacial catalysis for biodiesel production. *Green Chem.* **2017**, *19*, 4552–4562.
18. Chen, Z.; Ji, H.; Zhao, C.; Ju, E.; Ren, J.; Qu, X. Individual surface-engineered microorganisms as robust Pickering interfacial biocatalysts for resistance-minimized phase-transfer bioconversion. *Angew. Chem. Int. Ed. Engl.* **2015**, *54*, 4904–4908.
19. Liu, J.; Lan, G.J.; Peng, J.; Li, Y.; Li, C.; Yang, Q.H. Enzyme Confined in Silica-based Nanocages for Biocatalysis in Pickering Emulsion. *Chem. Commun.* **2013**, *49*, 9558–9560.
20. Scott, G.; Roy, S.; Abul-Haija, Y.M.; Fleming, S.; Bai, S.; Ulijn, R.V. Pickering stabilized peptide gel particles as tunable microenvironments for biocatalysis. *Langmuir* **2013**, *29*, 14321–14327.
21. Jiang, Y.; Liu, X.; Chen, Y.; Zhou, L.; He, Y.; Ma, L.; Gao, J. Pickering emulsion stabilized by lipase-containing periodic mesoporous organosilica particles: A robust biocatalyst system for biodiesel production. *Bioresour. Technol.* **2014**, *153*, 278–283.
22. Wang, L.; Liu, X.; Jiang, Y.; Zhou, L.; Ma, L.; He, Y.; Gao, J. Biocatalytic Pickering Emulsions Stabilized by Lipase-Immobilized Carbon Nanotubes for Biodiesel Production. *Catalysts* **2018**, *8*, 587.
23. Shi, J.; Wang, X.; Zhang, S.; Tang, L.; Jiang, Z. Enzyme-conjugated ZIF-8 particles as efficient and stable Pickering interfacial biocatalysts for biphasic biocatalysis. *J. Mater. Chem. B* **2016**, *4*, 2654–2661.
24. Chen, Z.; Zhao, C.; Ju, E.; Ji, H.; Ren, J.; Binks, B.P.; Qu, X. Design of Surface-Active Artificial Enzyme Particles to Stabilize Pickering Emulsions for High-Performance Biphasic Biocatalysis. *Adv. Mater.* **2016**, *28*, 1682–1688.
25. Moon, D.S.; Lee, J.K. Formation of wrinkled silica mesostructures based on the phase behavior of pseudoternary systems. *Langmuir* **2014**, *30*, 15574–15580.
26. Yang, W.; Li, B. A novel liquid template corrosion approach for layered silica with various morphologies and different nanolayer thicknesses. *Nanoscale* **2014**, *6*, 2292–2298.
27. Du, X.; Qiao, S.Z. Dendritic silica particles with center-radial pore channels: Promising platforms for catalysis and biomedical applications. *Small* **2015**, *11*, 392–413.
28. Zhou, W.J.; Fang, L.; Fan, Z.; Albela, B.; Bonneviot, L.; De Campo, F.; Pera Titus, M.; Clacens, J.M. Tunable catalysts for solvent-free biphasic systems: Pickering interfacial catalysts over amphiphilic silica nanoparticles. *J. Am. Chem. Soc.* **2014**, *136*, 4869–4872.
29. Fihri, A.; Bouhrara, M.; Patil, U.; Cha, D.; Saih, Y.; Polshettiwar, V. Fibrous Nano-Silica Supported Ruthenium (KCC-1/Ru): A Sustainable Catalyst for the Hydrogenolysis of Alkanes with Good Catalytic Activity and Lifetime. *ACS Catal.* **2012**, *2*, 1425–1431.
30. Park, D.S.; Yun, D.; Choi, Y.; Kim, T.Y.; Oh, S.; Cho, J.-H.; Yi, J. Effect of 3D open-pores on the dehydration of n-butanol to di-n-butyl ether (DNBE) over a supported heteropolyacid catalyst. *Chem. Eng. J.* **2013**, *228*, 889–895.
31. Du, X.; He, J. Amino-functionalized silica nanoparticles with center-radially hierarchical mesopores as ideal catalyst carriers. *Nanoscale* **2012**, *4*, 852–859.
32. Bouhrara, M.; Ranga, C.; Fihri, A.; Shaikh, R.R.; Sarawade, P.; Emwas, A.H.; Hedhili, M.N.; Polshettiwar, V. Nitridated Fibrous Silica (KCC-1) as a Sustainable Solid Base Nanocatalyst. *ACS Sustain. Chem. Eng.* **2013**, *1*, 1192–1199.
33. Li, K.; Wang, J.; He, Y.; Abdulrazaq, M.A.; Yan, Y. Carbon nanotube-lipase hybrid nanoflowers with enhanced enzyme activity and enantioselectivity. *J. Biotechnol.* **2018**, *281*, 87–98.
34. Zhang, L.; Ma, Y.; Wang, C.; Wang, Z.; Chen, X.; Li, M.; Zhao, R.; Wang, L. Application of dual-enzyme nanoflower in the epoxidation of alkenes. *Process Biochem.* **2018**, *74*, 103–107.
35. Shu, Q.; Gao, J.; Nawaz, Z.; Liao, Y.; Wang, D.; Wang, J. Synthesis of biodiesel from waste vegetable oil with large amounts of free fatty acids using a carbon-based solid acid catalyst. *Appl. Energy* **2010**, *87*, 2589–2596.
36. Halim, S.; Harunkamaruddin, A. Catalytic studies of lipase on FAME production from waste cooking palm oil in a tert-butanol system. *Process Biochem.* **2008**, *43*, 1436–1439.

37. Fan, Y.; Wu, G.; Su, F.; Li, K.; Xu, L.; Han, X.; Yan, Y. Lipase oriented-immobilized on dendrimer-coated magnetic multi-walled carbon nanotubes toward catalyzing biodiesel production from waste vegetable oil. *Fuel* **2016**, *178*, 172–178.
38. Dizge, N.; Aydiner, C.; Imer, D.Y.; Bayramoglu, M.; Tanriseven, A.; Keskinler, B. Biodiesel production from sunflower, soybean, and waste cooking oils by transesterification using lipase immobilized onto a novel microporous polymer. *Bioresour. Technol.* **2009**, *100*, 1983–1991.
39. Hakalin, N.L.S.; Molina-Gutierrez, M.; Prieto, A.; Martinez, M.J. Optimization of lipase-catalyzed synthesis of beta-sitostanol esters by response surface methodology. *Food Chem.* **2018**, *261*, 139–148.
40. Zhou, Z.; Inayat, A.; Schwieger, W.; Hartmann, M. Improved activity and stability of lipase immobilized in cage-like large pore mesoporous organosilicas. *Microporous Mesoporous Mater.* **2012**, *154*, 133–141.
41. Zhao, B.; Liu, X.; Jiang, Y.; Zhou, L.; He, Y.; Gao, J. Immobilized lipase from Candida sp. 99–125 on hydrophobic silicate: Characterization and applications. *Appl. Biochem. Biotechnol.* **2014**, *173*, 1802–1814.
42. Lee, H.V.; Yunus, R.; Juan, J.C.; Taufiq-Yap, Y.H. Process optimization design for jatropha-based biodiesel production using response surface methodology. *Fuel Process. Technol.* **2011**, *92*, 2420–2428.
43. Kumar, D.; Nagar, S.; Bhushan, I.; Kumar, L.; Parshad, R.; Gupta, V.K. Covalent immobilization of organic solvent tolerant lipase on aluminum oxide pellets and its potential application in esterification reaction. *J. Mol. Catal. B Enzym.* **2013**, *87*, 51–61.
44. Ngai, T.; Jiang, H.; Li, Y.; Hong, L. Submicron Inverse Pickering Emulsions for Highly Efficient and Recyclable Enzymatic Catalysis. *Chem. Asian J.* **2018**, *13*, 3533–3539.
45. Gao, J.; Kong, W.; Zhou, L.; He, Y.; Ma, L.; Wang, Y.; Yin, L.; Jiang, Y. Monodisperse core-shell magnetic organosilica nanoflowers with radial wrinkle for lipase immobilization. *Chem. Eng. J.* **2017**, *309*, 70–79.
46. Sheldon, R.A.; van Pelt, S. Enzyme immobilisation in biocatalysis: Why, what and how. *Chem. Soc. Rev.* **2013**, *42*, 6223–6235.
47. Yang, X.; Wang, Y.L.; Bai, R.X.; Ma, H.L.; Wang, W.H.; Sun, H.J.; Dong, Y.M.; Qu, F.M.; Tang, Q.M.; Guo, T.; et al. Pickering Emulsion-Enhanced Interfacial Biocatalysis: Tailored Alginate Microparticles Act as Particulate Emulsifier and Enzyme Carrier. *Green Chem.* **2013**, *21*, 2229–2233.
48. Zhang, C.; Hu, C.; Zhao, Y.; Moller, M.; Yan, K.; Zhu, X. Encapsulation of laccase in silica colloidosomes for catalysis in organic media. *Langmuir* **2013**, *29*, 15457–15462.
49. Jiang, Y.J.; Gu, H.Q.; Zhou, L.Y.; Cui, C.C.; Gao, J. Novel in Situ Batch Reactor with a Facile Catalyst Separation Device for Biodiesel Production. *Ind. Eng. Chem. Res.* **2012**, *51*, 14935–14940.